Research Article

iMedPub Journals
www.imedpub.com

Journal of Organic & Inorganic Chemistry
ISSN 2472-1123

2021
Vol.7 No.5:8106

Mixed Oxides of Cerium and Manganese as Catalysts for Total Oxidation of Ethyl Acetate: Effect of Preparation Procedure

Gloria Issa[1*], Momtchil Dimitrov[1], Radostina Ivanova[1], Martin Kormunda[2], Jiří Henych[3,4], Jakub Tolasz[4], Daniela Kovacheva[5], Tanya Tsoncheva[1]

[1]*Institute of Organic Chemistry with Centre of Phytochemistry, Bulgarian Academy of Sciences, Akad. G. Bontchev Str. Bl. 9, Sofia, Bulgaria*

[2]*Faculty of Science, J.E. Purkyně University, Pasteurova 3632/15, 400 96 Ústí nad Labem, Czech Republic*

[3]*Institute of Inorganic Chemistry of the Czech Academy of Sciences, 25068 Řež, Czech Republic*

[4]*Faculty of the Environment, University of Jan Evangelista Purkyně, Pasteurova 3632/15, 400 96 Ústí nad Labem, Czech Republic*

[5]*Institute of General and Inorganic Chemistry, Bulgarian Academy of Sciences, Sofia, Bulgaria, Akad. G. Bontchev Str. Bl 11, Sofia, 1113, Bulgaria*

[*]**Corresponding author:** Gloria Issa, Institute of Organic Chemistry with Centre of Phytochemistry, Bulgarian Academy of Sciences, Akad. G. Bontchev Str. Bl. 9, Sofia, Bulgaria, Tel: 0884140868; Email: issa@abv.bg

Received date: April 06, 2020; **Accepted date:** September 06, 2021**; Published date:** September 15, 2021

Citation: Issa G (2021) Mixed Oxides of Cerium and Manganese as Catalysts for Total Oxidation of Ethyl Acetate: Effect of Preparation Procedure. J Org Inorg Chem Vol: 7 No: 5.

Abstract

The microstructure of manganese and cerium oxide bi-component materials with different Ce/Mn ratio, obtained by co-precipitation and temlate assisted hydrothermal techniques, is studied in details by Nitrogen physisorption, XRD, SEM, TEM, XPS and Raman spectroscopies and TPR with hydrogen. The catalytic behaviour of the composites in total oxidation of ethyl acetate is investigated. It is found that the close contact between manganese and cerium metal oxide nanoparticles is realized by interface layer of isomorphously substitituted or incorporated in interstitial positions in ceria lattice manganese ions in different oxidative state. The physicochemical data evidence that this interface layer stabilizes a „shell“ of finely dispersed CeO2 species on the „core“ of MnOx entities, which plays a deciseve role in the catalytic process.

Keywords: Manganese and cerium metal oxide nanoparticles; Interface layer; Total oxidation of ethyl acetate.

Introduction

Volatile organic compounds (VOCs) are among the most noxious air pollutants due to their toxic nature and participation in smog formation. Among the various techniques for VOCs elimination, the catalytic combustion is the most promising and effective approach as it works at comparatively low temperatures and shows high selectivity that could lead to considerable environmental and economic benefits [1-4]. The synthesis and characterization of novel multicomponent nanosized materials have intensively been investigated in the recent years because of their wide application in various fields, and in particular in the field of catalysis [5-10]. The requirements for these materials are high, both for their activity, selectivity and stability during operation, as well as from an economic point of view – their low cost and ability to operate at relatively low temperatures. These issues are in the focus of many studies and patents in which innovative porous materials based on transition metals and nanosized metal oxides were used [10, 11]. They are one of the most important and widely used categories of solid catalysts that could be used both as active phases and supports. At the same time, ceria based catalysts are considered as very suitable candidates for the purpose due to the excellent redox properties of ceria resulting from the fact that both Ce4+ and Ce3+ are stable, thus allowing the oxide to readily shift between CeO2 and CeO2-x. Besides, the relatively easy introduction of another metal in the ceria lattice can increase the concentration of oxygen vacancies and thus further improve its oxygen-storage release capacity. A suitable candidate of such metal promoter is manganese and its addition to ceria could lead to the formation of a Ce-Mn oxide solid solution, however, the preparation method used could influence the structural, textural and catalytic properties of the obtained mixed oxide material. Large scale applications in various catalytic processes [12-18] of nanosized mesoporous ceria-manganesia have favored the development of various chemical methods for this binary oxide preparation including sol-gel techniques [15], thermal decomposition [16], micro-emulsion procedures [17], co-precipitation [18, 19, 20] and surfactant template method [21, 22]. Their catalytic activity can be traced from the presence of partially filled d-layers of the metal ion to the influence of the oxygen ligand field on these partially filled d-layers [12, 14]. The high catalytic activity is mainly associated with the favorable role of the manganese dopant leading to: decrease in particle size [13-18]; strong positive effect on the redox behaviour of the metal oxides [14-16]; high degree of synergistic interaction between the components [16-20], formation of solid solution and favorable modification of the structural and catalytic properties [13-18, 21]. It has been reported that the isomorphous incorporation of manganese ions in different oxidation states into the CeO2 lattice would lead to the

formation of solid solution with a high degree of defectness [16]. The formation of an optimal electronic structure may favor the realization of facilitated redox processes with enhanced electron mobility [20-25]. The use of various synthesis methods for preparation of Ce-Mn mixed oxide will contribute to the optimization of the particle sizes and the creation of materials with different morphology, high specific surface area and well-developed porous structure comprised of pores of different size, shape and topology [23, 24]. The use of hydrothermal treatment in the presence of structure-directing agents (templates) will result in materials with mesoporous structure and thicker walls, which will make them significantly more stable and could improve their catalytic activity by the formation of a large and well-exposed active surface and hence to facilitated access of the reactants to the catalytic active sites [25, 26].

The current investigation is focused on the preparation and characterization of series of cerium-manganese mixed oxides by two different but easy to implement procedures and their application as catalysts for ethyl acetate total oxidation, as one of the most difficult to completely oxidize VOC pollutant. The elucidation of the relation between the preparation procedure used and the structure, texture, morphology, surface and catalytic properties of the obtained materials was the main challenge in the study. For the purpose, the obtained materials were characterized by a complex of different physicochemical techniques, such as nitrogen physisorption, XRD, SEM, TEM, Raman and XPS spectroscopies and TPR with hydrogen.

Experimental

Materials: A series of cerium-manganese oxide samples were synthesized by template-assisted technique using N-cetyl-N,N,N-trimethyl ammonium bromide (CTAB, ≥99.0%, Merck) as a template and hydrothermal treatment at 373 K. For the purpose, 12.0 g CTAB were dissolved in 100 ml distilled water and then slowly and under vigorous stirring a second solution of CeCl3.7H2O (10.8 g) and/or MnCl2.4H2O (5.8 g) in different proportion (xCe:yMn, x:y mol ratio was 0:1, 1:2, 1:1, 2:1, 1:0) in 50 ml distilled water was added. Then, the temperature was raised to 323 K and the reaction mixture was stirred for 30 min before adding drop-wise 20 ml NH4OH (25 %). The resulting mixture was stirred overnight at 323 K and then transferred into suitable containers and hydrothermally treated at 373 for 24 h. The obtained materials were filtrated, washed copiously with distilled water, dried at room temperature and calcined with 1 K per minute up to 773 K, and then dwelled for 10 h at the final temperature. They were designated as xCeyMn-HT, where x and y indicate the mol ratio between Ce and Mn. Alternatively, the same series of samples, denoted as xCeyMn-CP was obtained using co-precipitation technique. For the purpose, 1M NH3 solution was added to an aqueous solution containing certain amounts of Mn(NO3)2.4H2O and/or Ce(NO3)2.6H2O until the pH of the solution reaches pH of 9. After 1 h of stirring the resulting precipitate was filtered, washed with distilled water and dried at 373 K for 24 hours. The oxide samples were obtained after calcination in ambient atmosphere at 773 K for 5 hours.

Methods of characterization: The texture characteristics of the obtained materials were studied by nitrogen sorption measurements on a Quantachrome NOVA 1200e instrument at 77 K. Powder X-ray diffraction patterns were collected on Bruker D8 Advance diffractometer equipped with Cu Kα radiation and LynxEye detector. The SEM images were obtained on FEI Nova NanoSEM 450 in a High-Vacuum mode using acceleration voltage of 5 kV. The morphology of the samples was measured on a FEI Talos F200X transmission electron microscope. Raman investigation was carried out on a DXR Raman microscope (Thermo Fischer Scientific, Inc., Waltham, MA) equipped with 532 nm laser. The surface chemical composition was investigated by X-ray photoelectron spectroscopy method (XPS) using a SPECS PHOIBOS 100 hemispherical analyzer with a 5-channel detector and a SPECS XR50 X-ray source equipped with an Al and Mg dual anode. The measurements were performed with Al anode at Epass 40eV for survey spectra and Epass 10eV for high resolution spectra. The TPR/TG (temperature-programmed reduction/ thermogravimetric) analyses were performed in a Setaram TG92 instrument. Typically, 40 mg of the sample were placed in a microbalance crucible and heated in a flow of 50 vol. % H2 in Ar (100°cm3min-1) up to 773 K at 5 Kmin-1 and a final hold-up of 1h.

Catalytic test: The total oxidation of ethyl acetate was carried out in a flow type reactor using 0.030 g of catalyst and a mixture of ethyl acetate in air (1.21 mol%), WHSV was 100 h−1. Before the catalytic experiments the samples were treated in argon at 373 K for 1 h and after testing the initial flow composition, the catalytic data were obtained under temperature programmed regime in the range of 470–773 K. Gas chromatographic analyses were performed on a HP 5890 apparatus using carbon-based calibration. The products selectivity was calculated as SCO2 for CO2, SAA for acetaldehyde, SEt for ethanol, SC2H4 for ethene and SAcAc for acetic acid by the equation: Si= Yi/X*100, where Si and Yi were the selectivity and the yield of (i) product and X was the conversion (50%). The specific catalytic activity (SA) was calculated as SA = X/A, where X was the conversion at 610 K and A was the specific surface area.

Results and discussion

XRD: In Fig. S1 are shown the XRD patterns of the samples obtained by different preparation procedures and the data for the phase composition, fluorite unit cell parameter and crystallite sizes of the samples are summarized in Table 1. In the case of analogous pure oxide samples no significant differences were registered. The diffraction peaks of 2θ centered at about 28.5°, 33.1°, 47.4°, and 56.4° were found in pure ceria catalysts and could be attributed to ceria with cubic fluorite crystallintiy (PDF2# 34-394) [11,12,15] with average crystallite size of about 17-18 nm (Table 1). The XRD patterns of pure manganese oxides contained intensive diffraction reflections at 2θ 23.1°, 33.1°, 38.2°, 55.2° and 65.9° 2Θ, corresponding to well crystallized Mn2O3 phase (PDF2# 41-1442) [16, 17, 20] with relatively large crystallites (Table 1). The characteristic diffraction peaks of Mn5O8 (PDF2# 39-1218) were observed at about 36.1°, 37.5° and 65.2° and about 18.1°, corresponding to Mn3O4 phase (about 10 %) in case of the HT sample, was also registered. No

diffraction peaks of manganese oxides are detected for the mixed oxides prepared by co-precipitation method (Fig. S1). In the case of mixed oxide samples (Fig. S1, Table 1) the CeO2 reflections are broader, lower in intensity and slightly shifted to higher Bragg angles as well. The broadening of the reflections indicates the decrease in the crystallite size of the fluorite-like phase, while the decrease in the reflections intensity together with their position shifting could be assigned to the incorporation of Mn ions in ceria lattice. Many authors also reported easy introduction of smaller manganese ions into the fluorite-like structure of CeO2 (the radius of Mn4+ is about 0.053 nm, Mn3+ is about 0.058 nm, Mn2+ is about 0.083 nm and the radius of Ce4+ is about 0.087 nm) [10-15, 23, 27]. The observed variations in the lattice parameter with the change in the method of preparation and the Ce/Mn ratio (Table 1) suggest differences in the degree of incorporation of Mn in the fluorite lattice.

Table 1: Phase composition, unit cell parameters, average crystallite size, BET surface area and total pore volume for all cerium and manganesium oxide materials.

Sample	Phase composition	Fluorite unit cell	SBET,	Vp,	D	Size
	(space group)		m2/g	cc/g	nm	nm
CeO2-CP	CeO2 (Fm-3 m)	5.413	48	0.12	7	17
CeO2-HT	CeO2 (Fm-3 m)	5.415	33	0.14	4	18
2Ce1Mn-CP	CeO2 (Fm-3 m)	5.409	82	0.2	5	15
2Ce1Mn-HT	CeO2 (Fm-3 m)	5.397	78	0.24	11	7
1Ce1Mn-CP	CeO2 (Fm-3 m)	5.408	67	0.21	16	10
1Ce1Mn-HT	84 % CeO2 (Fm-3 m)	5.334	66	0.47	28	7
	12% Mn5O8 (C2/m)					
	4% Mn2O3 (Ia-3)					
1Ce2Mn-CP	CeO2 (Fm-3 m)	5.409	58	0.26	17	12
1Ce2Mn-HT	69 % CeO2 (Fm-3 m)	5.335	65	0.37	17	6
	24% Mn5O8 (C2/m)					65
	7% Mn2O3 (Ia-3)					54
MnxOy-CP	40 % Mn2O3 (Ia-3)		6	0.05	4	56
	60 % Mn5O8 (C2/m)					25
MnxOy-HT	24 % Mn2O3 (Ia-3)		7	0.03	4	85
	67 % Mn5O8 (C2/m)					33
	9%Mn3O4 (I41/amd)					66

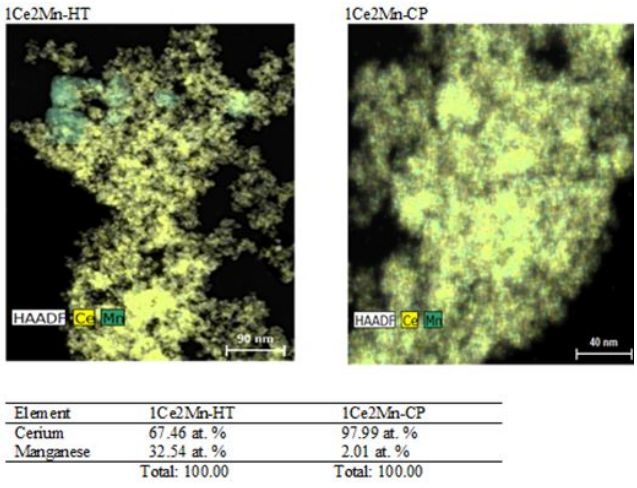

Nitrogen physisorption: Nitrogen physisorption analysis revealed the formation of mesoporous materials with relatively high specific surface areas (40-70 m2/g), broad pore size distribution and pore volumes within the range of 0.1-0.5 cc/g (Table 1). The appearance of a hysteresis loop above 0.8 relative pressure (Figure 1) suggests the existence of mesopores with irregular shape that are formed by interparticle interaction. Despite the preparation procedure used, the obtained binary oxides possess higher specific surface area as compared to the individual oxides (Table 1). The texture of the HT samples shows slightly higher BET surface area compared to the CP materials.

Figure 1: Nitrogen physisorption isotherms (a, b) and pore size distribution (c and d) of cerium and manganesium oxide materials obtained by hydrothermal and co-precipitation techniques.

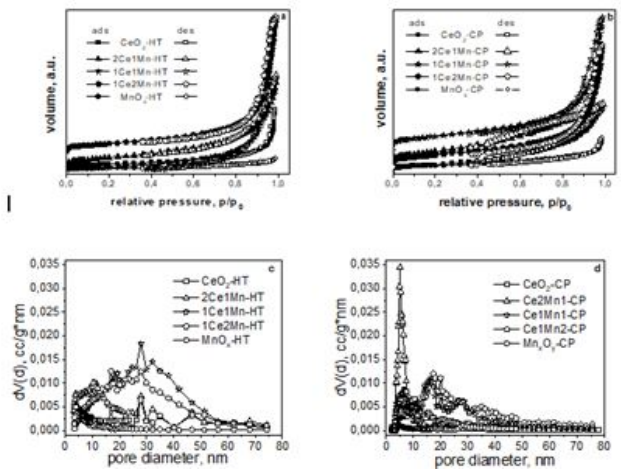

SEM and TEM analysis: The morphology of the samples was visualized by SEM micrographs (Figure 2). The SEM images of the CP oxides demonstrate presence of smaller and uniform particles for both mono- and bi-component materials. More significant changes in the morphology with the samples composition are observed for the HT materials. The small additives of Mn to ceria proviides the formation of needle-like structures (sample 2Ce1Mn-HT), the eqimollar ratio facilitates the formation of homogemneous phase, while the increase of Mn content 1Ce2Mn-HT leads to segregation of larger, probably MnxOy, particles. These results are in good correlation with the data from the XRD analyses (Table 1). The microstructure of the selected binary samples (1Ce2Mn-HT and 1Ce2Mn-CP) is characterized by the HAADF TEM images (Figure 3). As shown, the samples consist of finely dispersed nanoparticles with sizes similar to those obtained by XRD analysis, about 10 nm for 1Ce2Mn-CP sample and less than 10 nm in combination with bigger manganese oxide particles between 50 and 80 nm for 1Ce2Mn-HT, (Figure 3, Table 1). The quantative estimation of Ce and Mn surface distribution (Figure 3) shows that in both samples cerium is exposed at the surface, which for the CP sample is approximatelly 100 %.

Figure 2: SEM images of the obtained composites.

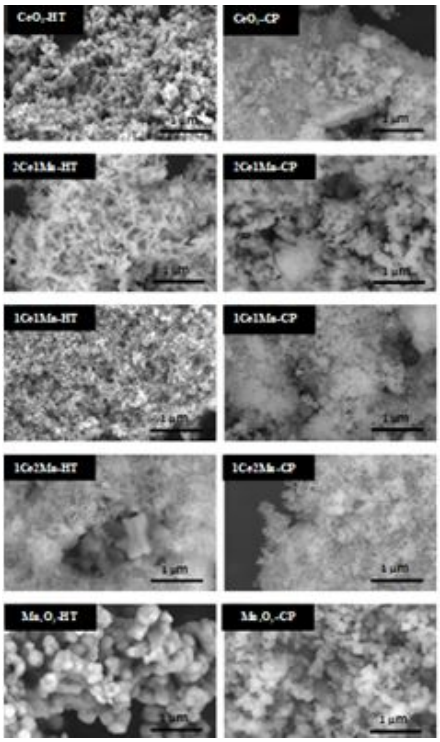

Figure 3: HRTEM, SAED and elemental distribution for 1Ce2Mn-HT and 1Ce2Mn-CP.

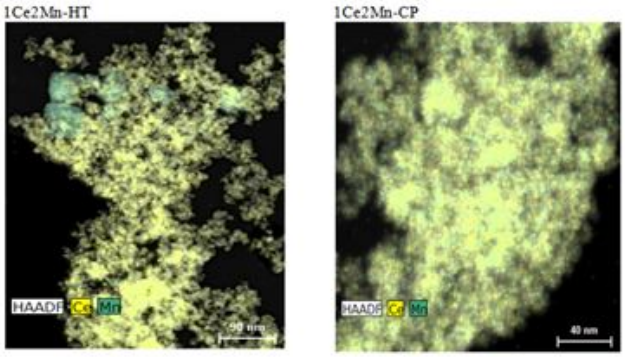

Element	1Ce2Mn-HT	1Ce2Mn-CP
Cerium	67.46 at. %	97.99 at. %
Manganese	32.54 at. %	2.01 at. %
	Total: 100.00	Total: 100.00

Raman and XPS analyses: Raman spectroscopy is an efective method to study the phase composition and the the changes in ions environment (Figure 4). For the pure ceria materials, the strong peak at 462 cm−1 is associated with the triply degenerate F2g Raman active mode for CeO2 fluorite structure, while the registered broad shoulder at about 600 cm-1 is due to the presence of oxygen defects [12, 15, 28]. Here, no certain differences between the HT and CP samples are observed. For the pure manganese oxides, the Raman shifts at 640 cm−1 is due to the Mn-O-Mn stretching mode in MnxOy phases [12, 15, 29]. Presence of well crystallized manganese oxide phase is observed in higher extent for the HT obtained analogues, which is in consistence with the XRD (Table 1) and SEM (Fig.2) data. The Raman shifts change significantly in case of all bi-component materials. A significant decrease in the intensity of F2g Raman active mode for CeO2, combined with its broadening and shifting to lower values was registered (Figure 4). The intensity

of the MnxOy Raman shifts also decreases significantly and this effect is most pronounced for the CP obtained binary materials. Note also the increase of the peaks at around 600 cm-1 for all bi-component materials, which is also observed in higher extent for the CP samples. In accordance with [12, 15] all these changes indicate penetration of Mn ions within ceria lattice, which is accompanied with the formation of oxygen deffects.

Figure 4: Raman spectra of cerium and manganesium oxide materials.

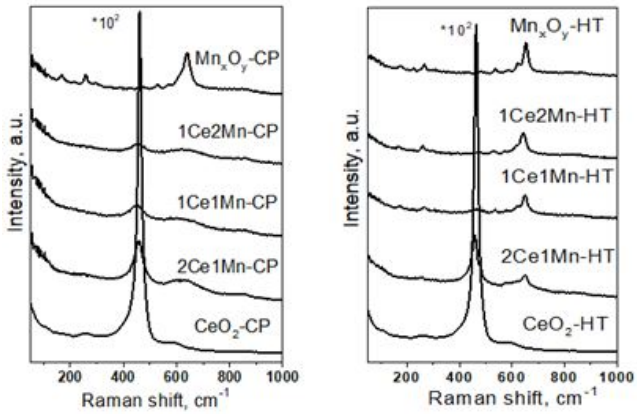

To precise the surface composition of the samples, XPS analyses are done. The Ce 3d and Mn 2p spectra are demonstrated in Fig. S2 and data for the samples composition are listed in Table 2. In the high resolution Ce 3d spectra (Fig. S2), the peaks at about 917.5, 907.8, 900.7, 898.6, 888.7 and 882.8 eV are assigned to Ce4+ ions, while the peaks at 903.5 and 884, 3 eV are typical of Ce3+ ions (Table 2) [15, 29, 30]. In the XPS spectra of Mn 2p (Fig. S2), the peaks around 640.1-641.6 eV and 651.7-652.3 eV are assigned to Mn3+ [31, 32], while the peaks around 640.7-642.8 and 652.3-654.6 eV are assigned to Mn4+ (Table 2) [31]. The domination of Ce4+ is detected for all binary materials. Typically the Ce3+ content is about 10-12 % and it remains almost the same despite the variations in the Ce/Mn ratio in the samples (Table 2). Just the opposite, significant changes are observed in the Mn ions distributions. The domination of Mn2+ and Mn3+ is found for the CP samples, and the relative part of the latter increases with the increase of Mn content in the samples. Almost similar distribution of Mn4+, Mn3+ and Mn2+, which proportion is not significantly changed with the Ce/Mn ratio in the samples, is detected for the HT prepared samples. All these data indicate stabilization of Mn ions in different oxidative states, probably due to their penetration within the ceria lattice. The variations in the proportion of Mn ions in different oxidative state for both series of samples could be due to different degree of incorporation of Mn ions, which is controlled by the preparation procedure and the Ce/Mn ratio itself. Note that the surface Ce/Mn ratio, obtained by XPS analyses (Table 2) is higher than the theoretical expected ratio. This evidences the high degree of exposure of cerium at the surface, in consistence with the results obtained from the TEM analyses (Figure 3).

Table 2: Surface area elemental composition from XPS analyses for mixed cerium and magnesium oxide materials. The used photoelectrons are indicated and RSF were used from CasaXPS library.

Sample	Atomic Concentration [at.%] Relative amount of states [%]				
	Ce (Ce 3d)	Mn (Mn 2p)	O (O 1s)	Mn4+ : Mn3+ : Mn2+	Ce4+ : Ce3+
2Ce1Mn-CP	30	2	65	18 : 15 : 66	90 : 10
2Ce1Mn-HT	27	4	65	low signal	88 : 12
1Ce1Mn-CP	25	5	64	8 : 53 : 38	82 : 18
1Ce1Mn-HT	23	9	65	26 : 35 : 38	87 : 13
1Ce2Mn-CP	21	7	62	16 : 55 : 29	89 : 11
1Ce2Mn-HT	16	12	64	28 : 35 : 37	89 : 11

TPR-TG analyses: TPR-TG profiles of the co-precipitated and the hydrothermally obtained Ce-Mn samples are presented in (Figure 5). The reduction of pure CeO2, prepared by HT and CP procedure was initiated just above 650 K and with further temperature increase up to 773 K corresponded to about 12-14% reduction of Ce4+ to Ce3+ ions [12, 15, 27]. At the same time, certain differences are found for the pure manganese oxide samples. For CP manganese oxides, two well defined DTG effects are found that we could assign to the reduction of Mn3+ and Mn4+ ions to Mn2,5+ and the second high-temperature effect to the reduction of Mn3O4 to MnO [31, 33]. On the other hand, the reduction of hydrotermally obtained MnxOy sample seems to be hindered and the first effect is much smaller and not well defined which we assign to the presence of alredy formed Mn3O4 phase within this sample during preparation. In the case of the bicomponent oxide samples, the reduction effects from both series are shifted to lower temperatures and significantly changed in their shape (Figure 5). In accordance with the XPS and XRD data, it could be assigned to the increase in the MnxOy dispersion, changes in the Mn oxidative state as well as to the formation of shared Ce-O-Mn bonds, where the oxygen mobility is facilitated. These effects are more pronounced for the CP materials, where XRD, Raman and TEM analysis confirmed the formation of more homogeneous and finely dispersed manganese oxide phase.

Figure 5: TPR-TG (a) and TPR-DTG (b) profiles of cerium and manganesium oxide materials obtained by hydrothermal and co-precipitation techniques.

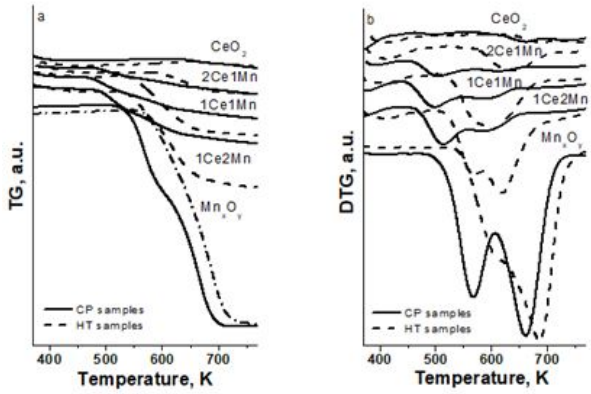

Catalytic test: (Figure 6) shows the catalytic activity in ethyl acetate oxidation for the obtained materials with different composition in a temperature-programmed regime. CO2, ethanol (Et), acetaldehyde (AA) and acetic acid (AcAc) in different proportions with reaction temperature increase were registered. For all samples, the catalytic activity was initiated above 500-550 K and the conversion steeply increases until a plateau-like region was reached above 600-650 K with 80-100% conversion combined with high CO2 selectivity, which is the desired final product for the total oxidation reaction. Among the pure metal oxides, both manganese oxide samples show similar and significantly higher conversion ability and selectivity to CO2 than the pure ceria samples (Figure 6). CeO2-HT demonstrates relatively low catalytic activity combined with low selectivity to CO2 due to the formation of ethanol as by-product. This result is not surprising taking into account that ethyl acetate oxidation is a stepwise process, including hydrolysis to ethanol and acetic acid and their further oxidation via Mars-van Krevelen mechanism [25, 26]. The first step is facilitated by the presence of acid sites, which formation in ceria seems to be promoted by the HT procedure. Mixed oxide materials show higher catalytic activity and high selectivity to CO2 than the pure oxides. This effect is typically assigned to higher concentration of oxygen vacancies [12, 15, 27], higher specific surface areas [12, 15], facilitated oxygen mobility (Fig. 5 and Table 2) [12, 13, 32] and the existence of strong interaction between ceria and manganese oxides (Figures 1 and 4, Table 2) [12-18]. In order to exclude the impact of the textural characteristics on the catalytic behaviour of the samples, the specific catalytic activity (SA) as a conversion per unit BET surface area is presented in Table 3. The SA for the pure MnxOy samples is extremely high and in contrast to our expectation, it was higher for the HT obtained sample, despite its lower dispersion (Table1, Figure 5). Note, that all binary materials demonstrate significantly lower SA.

Table 3: Products selectivity (%) for various samples in ethyl acetate oxidation at 50% conversion and specific activity per unit surface area at 610 K for cerium and manganesium oxide materials.

Sample	SBET, m2g-1	Conversion at 610 K, %	SA at 610 K	Products selectivity at 50 % conversion			
				SAA	SEt	SAcAc	SCO2
CeO2-CP	48	60	1.26	7	6	1	86
CeO2-HT	33	72	2.21	8	36	2	53
2Ce1Mn-CP	82	81	1.17	11	6	1	82
2Ce1Mn-HT	78	90	1.15	13	13	3	70
1Ce1Mn-CP	67	90	1.38	17	1	0	82
1Ce1Mn-HT	66	87	1.33	6	1	1	92
1Ce2Mn-CP	58	84	1.57	13	5	1	81
1Ce2Mn-HT	65	67	1.03	4	2	2	92
MnxOy-CP	6	88	14.9	12	2	0	86
MnxOy-HT	7	85	23.6	7	1	0	91

This evidences that the increase in the catalytic activity and selectivity in the binary materials is predominatly related to the improved textural characteristics of the samples. We would like to stress that the SA values for all binary materials are close to that one of pure cerium oxide. Remember, the higher Ce/Mn surface ratio as compared to the theoretical one, which was observed by SEM, TEM and XPS analyses. Thus, we can propose that the catalytic behaviour of the binary materials is mainly determined by the more accessible ceria species in it. The TPR measurements demonstrate facilitated oxygen mobility in all binary materials (Figure 5). At the same time, the XRD and Raman analyses show changes in the ceria lattice parameters, accompanied with the formation of oxygen deffects and disappearance of the crystalline MnxOy phase. Thus, formation of interface layer and/or solid solution, where the manganese ions are penetrated into the ceria lattice is assumed. The XPS data (Table 2) shows presence of manganese ions in different oxidation state. Relatively higher amount of Mn4+ is detected for the HT samples, while Mn2+, which amount decreases at the expense of the Mn3+ ions with the increase of Mn/Ce ratio, is observed for the CP ones. These varriations do not exclude changes in the solubility, and even in the mechanism of the insertion of Mn ions within the ceria lattice (interstitial or isomorphous substitution) with the variation of the preparation conditions and samples composition.

Figure 6: Ethyl acetate conversion (a, c) and selectivity to CO2 (b, d) of cerium and manganesium oxide materials obtained by hydrothermal and co-precipitation techniques.

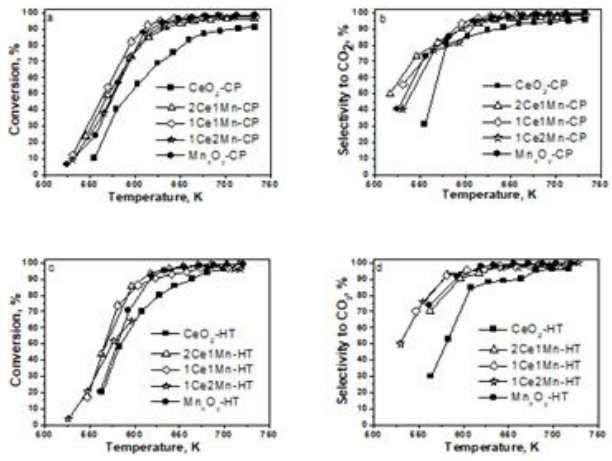

All these observations propose a „core-shell“ structure of the binary Ce-Mn oxide materialsis. Here, MnxOy stays as a „core“, covered by finely dispersed ceria species, which are stabilized by interface layer between them. The SEM, TEM, XPS, Raman and TPR analyses indicate that the formation of more homogeneous „core-shell“ structure is facilitated during the CP procedure, where the step-wise co-precipitation of the metal hydroxides is followed by the calcination at 773 K. It seems that the dehydroxilation of the precipitated hydroxides during the hydrothermal treatment at 373 K in the HT procedue provides penetration of Mn4+ ions within the ceria lattice in a high extent, but the next step of calcination at high temperature provokes segregation of MnxOy crystallites, and this is more pronounced with the increase of the Mn/Ce ratio in the samples.

Conclusion

The co-precipitated and template-assisted hydrothermally obtained Mn-Ce oxides represent a complex „core-shell“ structure, where finely dispersed ceria species are stabilized on the „core“ of MnxOy crystallites. An important role for the stabilization of the „core-shell“ structure plays the interface layer, where Mn ions in different oxidative state are penetrated within the ceria lattice, accompanied by the formation of oxygen vacancies. The preparation procedure and the Mn/Ce ratio are powerful approaches regulating the microstructure of these materials.

References

1. M. Konsolakis, S.A.C. Carabineiro, G.E. Marnellos, M.F. Asad, O.S.G.P. Soares, M.F.R. Pereira, J.J.M. Órfão, J.L. Figueiredo, Effect of cobalt loading on the solid state properties and ethyl acetate oxidation performance of cobalt-cerium mixed oxides, J. Colloid Interface Sci. 496 (2017) 141–149.
2. S. Cakmak, R.E. Dales, L. Liu, L.M. Kauri, C.L. Lemieux, C. Hebbern, J. Zhu, Residential exposure to volatile organic compounds and lung function: Results from a population-based cross-sectional survey, Environ. Pollut. 194 (2014) 145–151.
3. T. Garcia, B. Solsona, S.H. Taylor, The Oxidative Destruction of Hydrocarbon Volatile Organic Compounds Using Palladium–Vanadia–Titania Catalysts, Catal. Lett. 97 (2004) 99–103.
4. L. Hui, X. Liu, Q. Tan, M. Feng, J. An, Y. Qu, Y. Zhang, M. Jiang, Characteristics, source apportionment and contribution of VOCs to ozone formation in Wuhan, Central China, Atmos. Environ. 192 (2018) 55–71.
5. T. Seiyama, Total Oxidation of Hydrocarbons on Perovskite Oxides, Catal. Rev. 34 (1992) 281–300.
6. M.C. Álvarez-Galván, B. Pawelec, V.A. de la Peña O'Shea, J.L.G. Fierro, P.L. Arias, Formaldehyde/methanol combustion on alumina-supported manganese-palladium oxide catalyst, Appl. Catal. B 51 (2004) 83–91.
7. D. Zhang, X. Du, L. Shi, R. Gao, Shape-controlled synthesis and catalytic application of ceria nanomaterials, Dalton Trans. 41 (2012) 14455–14475.
8. S.S.T. Bastos, J.J.M. Órfão, M.M.A. Freitas, M.F.R. Pereira, J.L. Figueiredo, Manganese oxide catalysts synthesized by exotemplating for the total oxidation of ethanol, Appl. Catal. B: Environ. 93 (2009) 30–37.
9. C. Sun, H. Li, L. Chen, Nanostructured ceria-based materials: synthesis, properties, and applications,Energy Environ. Sci. 5 (2012) 8475–8505.
10. T. Montini, M. Melchionna, M. Monai and P. Fornasiero, , Fundamentals and catalytic applications of CeO2-based materials, Chem. Rev., 116 (2016) 5987–6041.